

Magnetic properties of NpGa₃ at high pressures

S. Zwirner

*European Commission, Joint Research Centre, Institute for Transuranium Elements, Postfach 2340, D-76125 Karlsruhe, Germany
and Physik-Department E-15, Technische Universität München, D-85747 Garching, Germany*

V. Ichas

European Commission, Joint Research Centre, Institute for Transuranium Elements, Postfach 2340, D-76125 Karlsruhe, Germany

D. Braithwaite

*Département de Recherche Fondamentale sur la Matière Condensée, SPSMS/LCP, CEA/Grenoble,
38054 Grenoble Cedex 9, France*

J. C. Waerenborgh

*European Commission, Joint Research Centre, Institute for Transuranium Elements, Postfach 2340, D-76125 Karlsruhe, Germany
and Department Química, ITN, 2686 Sacavém CODEX, Portugal*

S. Heathman

European Commission, Joint Research Centre, Institute for Transuranium Elements, Postfach 2340, D-76125 Karlsruhe, Germany

W. Potzel and G. M. Kalvius

Physik-Department E-15, Technische Universität München, D-85747 Garching, Germany

J. C. Spirlet and J. Rebizant

European Commission, Joint Research Centre, Institute for Transuranium Elements, Postfach 2340, D-76125 Karlsruhe, Germany

(Received 17 May 1996)

High-pressure studies on NpGa₃ were performed using ²³⁷Np Mössbauer spectroscopy, resistivity measurements, and x-ray diffraction, up to 9.2 GPa between 1.3 and 130 K, up to 25 GPa between 1.3 K and room temperature, and up to 40 GPa at room temperature, respectively. The cubic AuCu₃ crystal structure at ambient pressure is preserved up to 40 GPa. The bulk modulus B_0 is 75(2) GPa with $B'_0=6(2)$. NpGa₃ orders antiferromagnetically at ambient pressure at $T_N=67$ K. The magnetic ordering temperature increases up to ~ 200 K at 25 GPa. At 51 K and at ambient pressure a first-order antiferro- to ferromagnetic (AF-F) transition occurs with a sudden reduction of the magnetic hyperfine field B_{hf} by $\sim 15\%$ when entering the AF phase. At elevated pressure this transition is no longer observed. At 4.2 K B_{hf} , the value of the electric quadrupole coupling constant $|e^2qQ|$ and the isomer shift S slightly but continuously decrease with reduced volume. Above T_N a negative logarithmic resistivity slope $d\rho/d \ln T < 0$ is present at ambient pressure and disappears at 3 GPa. The slight decrease of B_{hf} at 4.2 K, the variation of e^2qQ and S with pressure, and the suppression of $d\rho/d \ln T$ at ~ 3 GPa indicate $5f$ electron delocalization. This delocalization, however, is much less pronounced than in band magnets, as, e.g., in NpOs₂. A magnetic phase diagram is suggested that consistently explains the pressure variation of ρ , B_{hf} and T_{ord} . We discuss the properties of NpGa₃ in terms of the Kondo interaction and the Doniach phase diagram, and alternatively, within a model which includes $5f$ electron delocalization effects. This second model seems to be promising. [S0163-1829(96)05241-1]

I. INTRODUCTION

The intermetallic compounds of the light actinides exhibit a wide variety of physical, especially magnetic, properties. The latter cover, for example, localized $5f$ magnetism, correlated $5f$ electron behavior, superconductivity and Pauli paramagnetism.¹ The UX₃ and NpX₃ compounds ($X=\text{Al, Ga, In, Tl, Si, Ge, Sn, Pb}$), all crystallizing in the AuCu₃ structure, provide an excellent possibility for an investigation of systematic changes in $5f$ electron structure.²⁻⁶ For example, USi₃, UAl₃, and UGe₃ are Pauli paramagnets.^{2,3} USn₃ exhibits strong spin fluctuations.⁷ UIn₃, UTl₃, and UPb₃ show features typical for localized systems, whereas

UGa₃ rather behaves like an ordered band magnet.³ It is less clear, however, which general model applies to describe the various electronic features of the NpX₃ compounds. For example, NpSn₃ was initially described as an itinerant system with a high density of $5f$ electrons at the Fermi level. This appeared to follow from susceptibility and specific-heat measurements, from the small ordered magnetic moment μ_{ord} of $0.3\mu_B$ (compared to a free ion value of $2.6\mu_B$), the low ordering temperature T_{ord} of 9.5 K, and from band-structure calculations.^{8,9} Unexpectedly, NpSn₃ behaves like many localized systems under pressure, i.e., T_{ord} rises strongly with reduced volume whereas μ_{ord} varies only slightly.^{10,11} To explain the pressure behavior typical for a localized f elec-

tron structure it was suggested that μ_{ord} is partially suppressed by Kondo interaction (“Kondo compensation”) rather than by $5f$ delocalization. At high temperature such a behavior is often connected with a Kondo anomaly of the resistivity,¹² i.e., a negative slope $d\rho/d \ln T < 0$ in the resistivity versus temperature curve, which has recently been observed for NpSn_3 .⁶

The pressure behavior of Kondo lattice systems is not well understood at present. Some models, for example the Doniach model,^{13–16} which extend the Kondo “impurity” case to Kondo lattices, successfully describe many Ce and light actinide intermetallics.^{17,18} According to these models, the hybridization of the localized f electrons with the conduction band leads to an antiferromagnetic spin exchange interaction J_h , which causes a negative logarithmic resistivity slope to appear at high temperature. In simple “impurity” models $d\rho/d \ln T$ is proportional to the third power of (J_h/W) ,^{15,16} where W is the width of the conduction band. The exchange interaction J_h also gives rise to a singlet ground state and competitively to a magnetic two ion interaction. Below a critical value $(J_h/W)_c$ magnetic order dominates. Above $(J_h/W)_c$ the Kondo mechanism leads to a singlet ground state, or at least partly suppresses μ_{ord} and weakens the magnetic order. Thus, if the volume dependence of J_h/W is known the volume dependence of μ_{ord} , T_{ord} , and of $|d\rho/d \ln T|$ can be qualitatively predicted and compared to experiment.

Surprisingly, for some actinide compounds which display a $d\rho/d \ln T$ anomaly, comparatively large ordered moments are reported. There are cases where the moments are even close to the free ion value or can be derived from the crystalline electric-field (CF) interactions without invoking the Kondo mechanism. Examples are NpAs ($2.5\mu_B$ as compared to $2.6\mu_B$ for Np^{3+}), NpSb ($2.6\mu_B$),^{19,20} UTe ($2.25(5)\mu_B$, compared to $3.4\mu_B$ for U^{3+} or $2.18\mu_B$ determined from a crystal-field model).^{21,22} Therefore the resistivity anomaly is not necessarily connected to a Kondo compensation of μ_{ord} . NpGa_3 is another example, where above T_{ord} (~ 67 K) (Ref. 23) a negative resistivity slope $d\rho/d \ln T$ appears. Between 67 and 50 K the magnetic structure is antiferromagnetic (AF). Below 50 K the moments are aligned ferromagnetically (F) with a saturation moment of $\sim 1.6\mu_B$. This is much larger than in NpSn_3 , but considerably smaller than the free-ion moment. At 50 K the F and AF phases coexist with the ordered moment reduced by $\sim 15\%$ in the AF phase.²³ The ambient pressure data available to date give no evidence which mechanism, e.g., $5f$ delocalization, Kondo compensation or CF interaction, causes the reduction of μ_{ord} relative to the free-ion value.

Since J_h/W is sensitive to volume changes we also intended to study at high pressures whether the magnetic parameters μ_{ord} and T_{ord} are correlated with $|d\rho/d \ln T|$ for NpGa_3 and whether the Doniach model applies. In this paper, we report on the results of ^{237}Np Mössbauer spectroscopy, resistivity, and x-ray-diffraction measurements at high pressures.

II. EXPERIMENTAL DETAILS

A. Sample preparation and characterization

The NpGa_3 sample was prepared by arc melting of stoichiometric amounts of neptunium and gallium metal in dry

argon gas. X-ray-diffraction patterns obtained with a Debye-Scherrer camera showed a pure cubic AuCu_3 phase (space group $Pm\bar{3}m$) with a lattice parameter of $a = 4.255 \text{ \AA}$. The sample quality was also checked by ^{237}Np Mössbauer spectroscopy between 1.3 and 140 K. The Mössbauer patterns observed in the paramagnetic phase show no quadrupole splitting and correspond to a single-phase material having cubic structure. At 4.2 K and ambient pressure the data agree well with the results of a previous investigation of NpGa_3 from a different batch.²³ We tried to reproduce the temperature variation of the magnetic hyperfine field published in Ref. 23, where at 50 K a coexistence of two magnetic sites has been reported [with the fields 285(3) T and 244(5) T]. We observe the same effect, however in a larger temperature range between 51(1) and 56(1) K. Our fields at 51 K agree well with the previous values. The ordering temperature of 67(1) K deviates only slightly from that of 65 K reported in Ref. 23.

B. Experimental methods

The compressibility studies were performed in a diamond-anvil cell of the Syassen-Holzapfel type²⁴ up to a pressure of 40 GPa. The sample was loaded into a 0.2 mm diameter hole of an Inconel gasket. Silicon oil was used as pressure transmitting medium. The pressure was measured on a ruby splinter within the sample chamber, according to the ruby fluorescence method.²⁵ The energy dispersive method was used for collection of x-ray data. Details of the set up are described in Ref. 26. All compressibility measurements were performed at room temperature.

Mössbauer transmission experiments on the 60 keV γ rays of ^{237}Np were carried out using a ^{241}Am metal source (about 50 mCi). The absorber was a powder sample with a thickness of $\sim 100 \text{ mg/cm}^2$ of ^{237}Np . It was compressed into a pellet of 4.5 mm diameter and 0.2 mm height and encapsulated in Al for radiation safety. The Al capsule (5 mm diameter, 0.7 mm height, 0.25 mm wall thickness) was mounted inside a high-pressure cell of the Bridgman type using B_4C anvils. The Al capsule and a small amount of paraffin between the capsule and the anvils served as pressure transmitting medium. The rather large absorber area restricted the pressure range to ~ 9 GPa. Pressure was applied to the cell inside a Cu-Be clamp at room temperature. The whole system was then mounted in a cryostat allowing absorber temperatures between 1.3 and 150 K. The source was always kept below 25 K. The pressure and pressure gradient were determined *in situ* with a Pb manometer making use of the pressure dependence of the superconducting transition temperature.²⁷ The pressure gradient was below 10%. Details of the Mössbauer high-pressure spectrometer can be found in Refs. 28 and 29.

The high-pressure resistivity measurements require very thin specimens ($\sim 0.8 \times 0.2 \times 0.03 \text{ mm}^3$). Due to the brittleness of NpGa_3 it is difficult to prepare a sample of the desired dimensions. Therefore small polycrystalline pieces were pressed in order to get 0.03 mm thin foils from which the sample was cut. The electrical resistance of the sample placed inside of a sintered diamond-anvil device was determined by the four-probe method. We used steatite as the pressure transmitting medium providing quasihydrostatic conditions. Successive cooling and heating cycles from 300

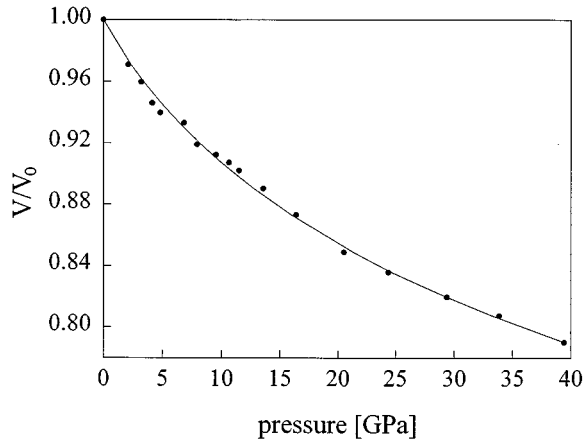


FIG. 1. Relative volume V/V_0 of the unit cell at room temperature as a function of pressure. The solid line is a fit to the Birch-Murnaghan equation.

down to 1.5 K were performed up to 25 GPa. The pressure was measured at low temperature using the superconducting transition of Pb similar to the Mössbauer experiments.

III. RESULTS

A. X-ray diffraction

Figure 1 shows the relative volume of the unit cell of NpGa₃ at room temperature as a function of pressure. The data were fitted with the Birch-Murnaghan equation of state³⁰ and gave values of the bulk modulus $B_0=75(2)$ GPa and its derivative $B'_0=6(2)$. These values are within errors the same as those found for NpSn₃ which were $B_0=72(10)$

GPa, $B'_0=6(4)$.³¹ No crystallographic phase transition was observed in NpGa₃ up to the maximum pressure of 40 GPa.

B. Mössbauer spectroscopy

Figure 2 shows Mössbauer spectra recorded at 4.2 K and above the ordering temperature at ambient pressure and at 9.2 GPa. The 4.2 K spectra were fitted assuming a single Np site with a combined magnetic hyperfine and collinear axially symmetric quadrupole interaction. Above T_{ord} we observe a single Lorentzian line. The results of the measurements at 4.2 K and for all pressures investigated are summarized in Table I. Its last column demonstrates the enormous increase of the ordering temperature with pressure. Figure 2 shows that at 4.2 K the magnetic hyperfine field changes only slightly when external pressure is applied. The additional line broadening is probably due to the pressure gradient in the cell which leads to a small distribution of the isomer shift. For all pressures investigated the magnetic hyperfine fields B_{hf} are plotted against temperature in Fig. 3. In Fig. 4 we show the pressure dependences of B_{hf} , the ordering temperature T_{ord} , and the isomer shift S .

The following major conclusions can be drawn:

(a) In the whole pressure range investigated there is no quadrupole splitting in the paramagnetic phase suggesting that the Np site symmetry remains cubic. Furthermore, at 4.2 K we observe no discontinuity of the isomer shift or the quadrupole interaction with pressure (see Fig. 4). We conclude that the AuCu₃ structure does not change up to 9 GPa. This is consistent with our room-temperature high-pressure x-ray data.

(b) The ordering temperature increases from 67 K at ambient pressure to 105 K at 9.2 GPa (see Fig. 4 and Table I).

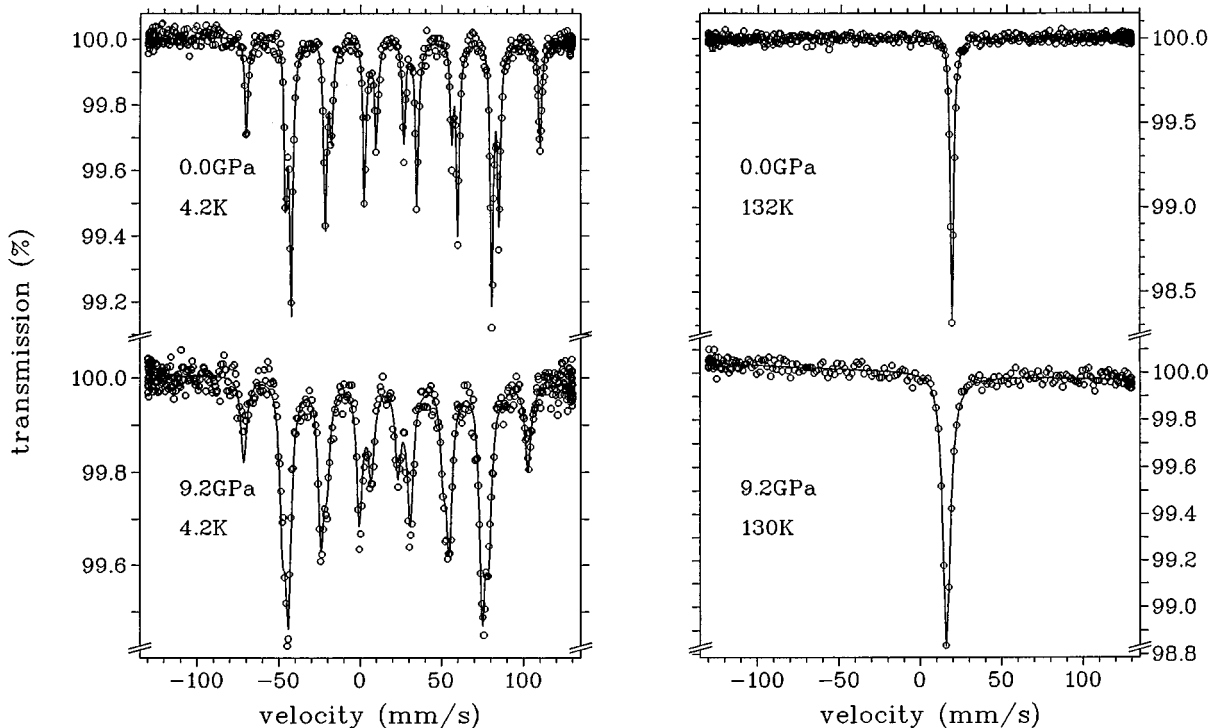


FIG. 2. Mössbauer spectra of NpGa₃ at 4.2 K and above the ordering temperature at ambient pressure and at 9.2 GPa.

TABLE I. Mössbauer results at 4.2 K for various pressures p . The magnetic hyperfine field B_{hf} , the coupling constant of the electric quadrupole interaction e^2qQ , the isomer shift S , and the linewidth Γ (full width at half maximum) are listed. The isomer shift is given relative to NpAl_2 . The last column gives the magnetic ordering temperature T_{ord} .

p (GPa)	B_{hf} (T)	e^2qQ (mm/s)	S (mm/s)	Γ (mm/s)	T_{ord} (K)
0.0	334(2)	-3.1(3)	5.9(2)	2.2(2)	67(2)
3.8(3)	333(2)	-2.8(4)	4.4(2)	3.7(2)	85(2)
4.8(3)	333(2)	-2.6(4)	3.8(2)	2.6(3)	91(2)
6.6(3)	329(2)	-1.6(4)	3.3(2)	3.8(3)	96(2)
7.7(3)	328(2)	-2.2(4)	2.3(2)	3.5(3)	100(2)
9.2(7)	323(2)	-1.5(4)	2.1(2)	4.3(3)	105(2)

(c) Contrary to the situation at ambient pressure where at 51 K two magnetic subspectra are found, we obtain under pressure spectra with only *one* magnetic hyperfine field in the whole temperature range below T_{ord} [see Fig. 3(a)]. Fur-

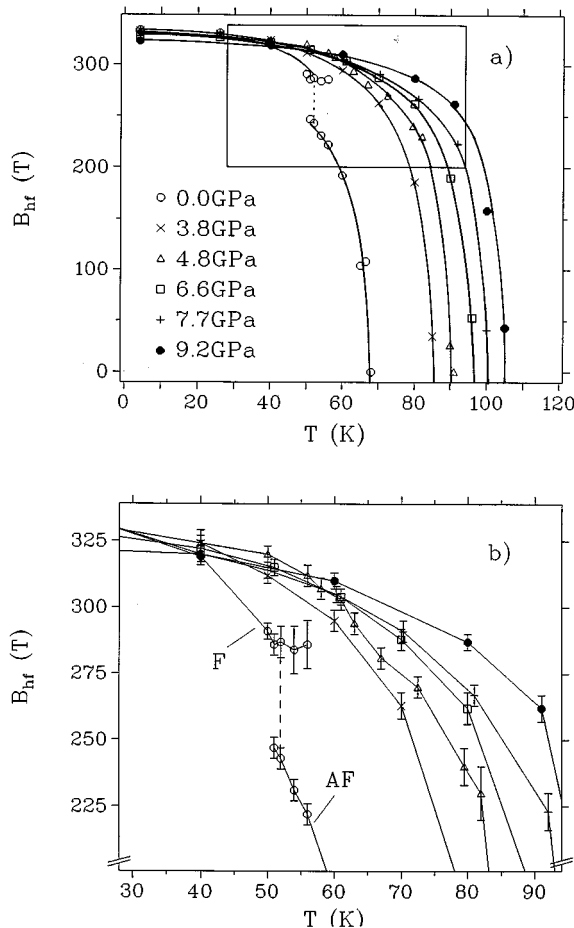


FIG. 3. Magnetic hyperfine field B_{hf} versus temperature T for various pressures. (a) For a better overall view error bars are not given. The solid lines serve as a guide to the eye. (b) The enlarged section shows that in contrast to ambient conditions, at elevated pressure no discontinuous drop of B_{hf} occurs at ~ 50 K within experimental errors. This drop is due to a transition from a ferromagnetic (F) to an antiferromagnetic (AF) state. Symbols have the same meaning as in (a).

thermore, within the experimental error the B_{hf} values at elevated pressure show no discontinuity as a function of temperature [see Fig. 3(b)]. Only the higher B_{hf} component attributed to the ferromagnetic phase at *ambient* pressure is present. Previous Mössbauer measurements at ambient pressure under external magnetic field³² showed an analogous effect. Above 50 K a magnetic field of ~ 4 T induces a change from the lower (“antiferromagnetic”) to the higher (“ferromagnetic”) B_{hf} value. Magnetization measurements revealed indeed that above 50 K a field of 4 T drives an antiferro- to ferromagnetic transition.²³

(d) At all pressures the magnetic hyperfine fields are saturated at 4.2 K (see Fig. 3). There is a slight decrease of B_{hf} by $\sim 3\%$ from ambient pressure to 9.2 GPa (see Fig. 4). The B_{hf} versus pressure curve reveals a negative curvature. The $B_{\text{hf}}(T)$ curves cannot be fitted by a Brillouin function. How-

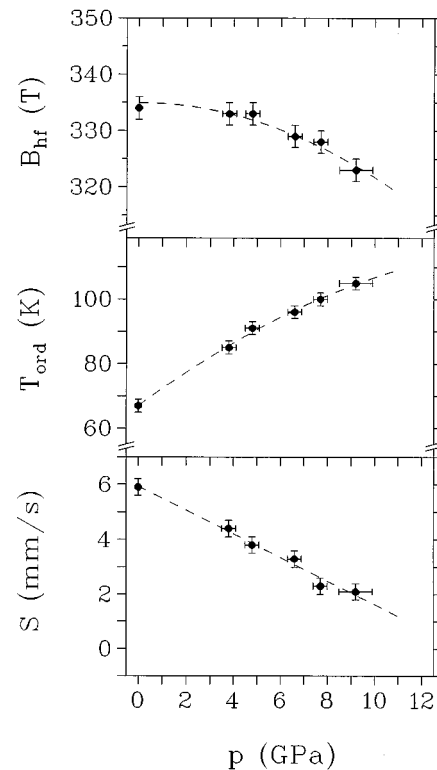


FIG. 4. Pressure dependences of the magnetic hyperfine field B_{hf} at 4.2 K, the ordering temperature T_{ord} , and the isomer shift S relative to NpAl_2 .

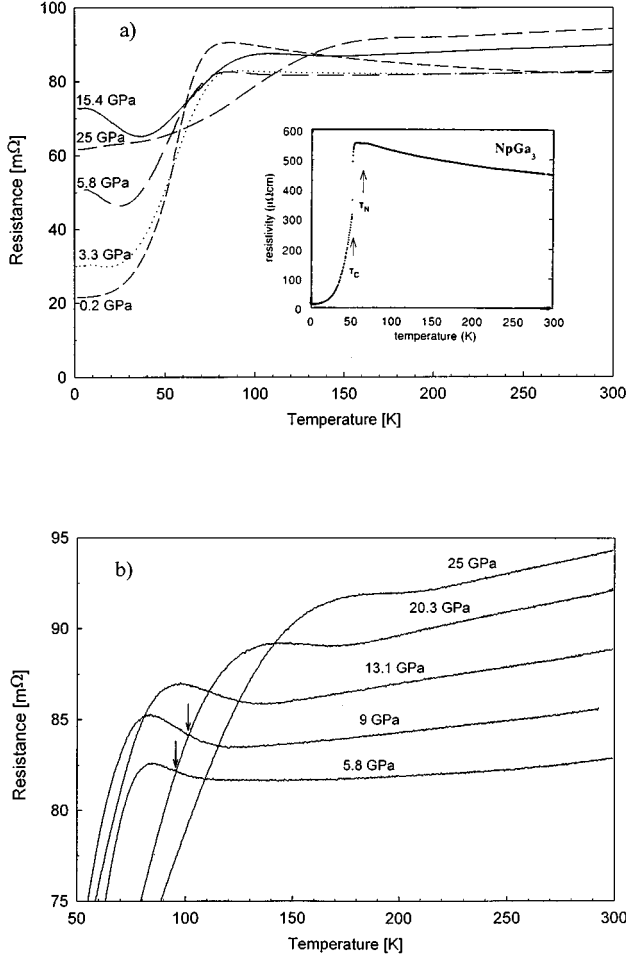


FIG. 5. Resistance versus temperature curves for various pressures. The inset in (a) shows the resistivity curve previously measured with a different sample (Ref. 23). The 0.2 GPa curve in (a) is normalized to the 3.3 GPa curve at room temperature (see text). The arrows in (b) indicate the inflection points which coincide with the ordering temperatures as derived from the Mössbauer measurements.

ever, at elevated pressures the magnetic hyperfine fields decrease continuously when temperature is raised suggesting that the magnetic phase transitions are of second order (see Fig. 3).

(e) The coupling constant e^2qQ of the quadrupole interaction at 4.2 K increases from $-3.1(3)$ mm/s at ambient pressure to $-1.5(4)$ mm/s at 9.2 GPa (see Table I), i.e., $|e^2qQ|$ is reduced under pressure. Such a behavior can be expected from the decrease of B_{hf} since at least part of e^2qQ is “induced:” it originates from the noncubic ground state of NpGa₃ when magnetically ordered.³³

(f) The isomer shift at 4.2 K shows a linear decrease under pressure (see Fig. 4) with a normalized slope of $(1/\Delta S_c)dS_c/dp=0.8\times 10^{-2}$ GPa⁻¹, where ΔS_c is the difference of S between the Np³⁺ and Np⁴⁺ configurations.³⁴ The value is somewhat larger than that found for NpSn₃ (0.6×10^{-2} GPa⁻¹).

C. Resistivity

Since the sample geometry is not well known, we use the resistance R rather than the specific resistivity ρ to present

the data. Some resistance curves $R(T)$ at various pressures are shown in Figs. 5(a) and 5(b). The resistivity curve previously obtained at ambient pressure²³ with a sample from a different batch is depicted in the inset of Fig. 5(a).

First we compare the $R(T)$ curve of our experiment at the lowest pressure (0.2 GPa) with the data obtained at ambient pressure. In both curves we observe above 100 K a logarithmic dependence of the resistance on T with a negative slope [see Fig. 5(a)]. The authors of Ref. 23 attributed this anomaly to the Kondo mechanism. Furthermore, both measurements reveal at ~ 50 K a steep decrease towards lower temperatures. At ambient pressure the drop coincides with the antiferromagnetic to ferromagnetic transition (AF-F).²³ However, whereas at ambient pressure $R(T)$ shows an almost discontinuous drop at T_C [inset of Fig. 5(a)] our measurement at 0.2 GPa displays a smooth behavior. Moreover, a small shoulder appearing at T_N in the ambient pressure curve is absent in our measurement. At present it is unclear whether the different features of the two measurements are a true pressure effect, whether they are due to imperfect conditions in the pressure cell (i.e., pressure gradient) or simply due to the different samples. Our Mössbauer data at ambient pressure show a coexistence of the two magnetic phases in a wide temperature range between 51 and 56 K (see Sec. II and Fig. 3). Therefore it might be not so surprising that we do not find a discontinuous drop of $R(T)$ at ~ 50 K.

In the following we concentrate on pressure effects and describe the changes of $R(T)$ when the applied pressure is higher than 0.2 GPa. At the initial increase in pressure, from 0.2 to 1.2 GPa, the sample resistance decreased by about a factor of 2 over the whole temperature range. At higher pressures the room-temperature resistance changes very little with pressure, and as none of our measurements suggest a cause for this major change between 0 and 1.2 GPa we suspect that this is not an intrinsic property but probably more the effect of pressure on grain boundaries and cracks in the polycrystalline sample. In Fig. 5(a) we have therefore normalized the 0.2 GPa curve to the 3.3 GPa curve at room temperature. Because of this limitation we will only focus on changes in the shape and position of the features in the curve, and not on absolute values of the resistance.

The logarithmic Kondo anomaly above T_{ord} weakens under pressure and disappears at 4.8 GPa. To estimate the behavior of the anomalous slope $b=-dR/d\ln T$ with pressure we fit the parameters a , b , and c of the function $R(T)=a-b\ln T+cT$ to the high-temperature (>100 K) resistance curves up to 3.3 GPa. The coefficient c represents the contribution of the electron phonon scattering.³⁵ The resulting b/a ratios are listed in Table II. The ratio of 0.09 at 0.2 GPa agrees well with the value of 0.1 previously found at ambient pressure.²³ Table II shows that b/a decreases continuously. At 4.8 GPa a $\ln T$ behavior could not be justified by the data.

In Fig. 6, the ordering temperature (\bullet) obtained from the Mössbauer data, T_{ord} (\blacksquare) as derived from the resistance curves, and the characteristic temperature of the resistance drop (Δ) are plotted against pressure (reduced volume). The position of the low-temperature drop (Δ), i.e., the temperature where the maximum of the derivative dR/dT appears, is almost pressure independent up to ~ 13 GPa. Above 13 GPa the drop is shifted from ~ 56 K at 13 GPa to ~ 90 K at 25 GPa. Between 5 and 9 GPa the position of the inflection point (\blacksquare) (the temperature where $d^2R/dT^2=0$) indicated by

TABLE II. b/a ratios obtained from fits of the function $R(T) = a - b \ln T + cT$ to the resistivity curves at high temperature and for various pressures p . Since the table is meant to show only trends, errors are not given.

p (GPa)	0.0	0.2	1.01	1.2	2.1	3.3	4.8
b/a	0.1 ^a	0.09	0.07	0.05	0.04	0.04	

^aReference 23.

an arrow in Fig. 5(b) coincides with the ordering temperatures (●) found in the Mössbauer measurements. Therefore, we believe that the inflection point is caused by the onset of magnetic order and indicates the magnetic phase transition also at higher pressures. A similar coincidence of a resistance inflection point with T_{ord} has been observed in NpP (Ref. 36) and Tb.³⁷ Above 10 GPa the temperature of the inflection point rapidly increases and reaches 194 K at 25 GPa, i.e., the ordering temperature probably rises correspondingly. Whereas the curvature of the T_{ord} versus pressure curve is negative between ambient pressure and 10 GPa, at higher pressures the slope increases and displays a linear dependence.

At low temperature and between 0.2 and 2.1 GPa we could fit the function $R(T) = R_0 + A \cdot T^2$ to the data. For ferromagnetically ordered systems the T^2 law is usually attributed to electron scattering at ferromagnetic spin waves.³⁵ The parameter A decreases by a factor of 10 between 0.2 and 2.1 GPa. Above 2.1 GPa the T^2 law can no longer be applied. Instead a minimum of $R(T)$ appears at ~ 20 K (see Fig. 5). The temperature of this minimum increases to ~ 37 K at 22 GPa. Furthermore, the resistance below 40 K increases between 0.2 and 15.4 GPa. At 25 GPa the minimum is no longer present, but the value of R at 1.5 K is still enhanced in comparison to 0.2 GPa. The origin of the minimum is not yet clear. We find no feature in the Mössbauer spectra, e.g., no change in the magnetic hyperfine field, which could be related to the minimum.

IV. DISCUSSION

We assume that the linear relation $B_{\text{hf}} = 215 \times \mu_{\text{ord}}$ between the magnetic hyperfine field B_{hf} (T) derived from

TABLE III. Volume coefficients of the electron density at the nucleus $\rho(0)$ derived from the isomer shift, of the ordered magnetic moment μ_{ord} , and of the magnetic ordering temperature T_{ord} . The arrow indicates the increase of $4f$ or $5f$ electron delocalization between DyAl₂ and NpOs₂ (see text).

Compound	$10^5 d \ln \rho(0) / -d \ln V$	$d \ln \mu_{\text{ord}} / -d \ln V$	$d \ln T_{\text{ord}} / -d \ln V$	
DyAl ₂ ^a	+5.6	+0.1	+5.3	Localized ↓ Delocalized
NpCo ₂ Si ₂ ^a	+2.4	+0.1	+7.0	
NpAs ^a	+4.2	-0.8	-1.3	
NpAl ₂ ^a	+5.0	-4.0	-16.0	
NpOs ₂ ^a	+12.5	-46.0	-80.0	
NpSn ₃ ^a	+1.7	+2.7 ^b	+9	
		-1.3 ^c		
NpGa ₃ ^d	+2.6	-0.1	+6	

^aReference 29.

^bBetween ambient pressure and 4.4 GPa.

^cBetween 4.4 and 6.2 GPa.

^dThis work.

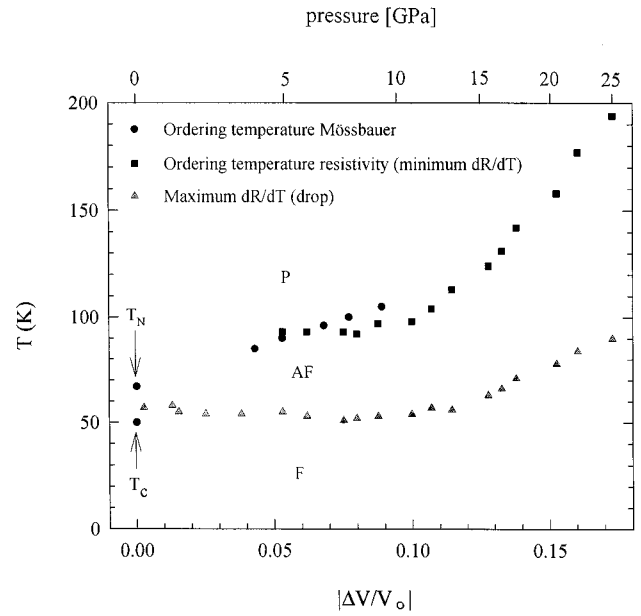


FIG. 6. The ordering temperatures deduced from Mössbauer spectroscopy (●) and from resistance measurement (■) versus pressure (volume reduction). The maximum of the derivative dR/dT of the low-temperature drop (Δ) is also plotted. Based on these data a magnetic phase diagram is proposed. The phase above the Néel temperature (●, ■, $T_N = 67$ K at ambient pressure) is paramagnetic (P). The antiferromagnetic phase (AF) is present between the Néel temperature (●, ■) and the temperature (Δ), which coincides with the resistance drop. Below Δ (T_C) the spin arrangement is proposed to be ferromagnetic (F). At ambient pressure T_C is ~ 50 K.

Mössbauer measurements and the ordered magnetic moment μ_{ord} (μ_B) determined by neutron diffraction also holds for NpGa₃ at ambient and at elevated pressure. The relation is well fulfilled for almost all Np intermetallics.³⁸

A. Localized versus itinerant $5f$ electron behavior

In the isostructural UGa₃ the weak temperature dependence of the magnetic susceptibility and the comparatively

TABLE IV. Important magnetic interactions for NpGa₃.

Interactions	Our assumption for NpGa ₃	Evidence from experiment	Future investigations
Intraionic correlation, CF state	RS-coupling dominant Np ³⁺ → ⁵ I ₄ → Γ ₅	Isomer shift → Np ³⁺ , μ _{ord} , e ² qQ → Γ ₅ , susceptibility (Ref. 23)	Experiment: inelastic neutron experiment theory: calculation within model II (Ref. 42)
Quadrupolar interaction	Weak	Small induced electr. field gradient	
Anisotropy of magnetic exchange	Weak		Theory: influence on CF state and on μ _{ord}
Hybridization exchange J _h	Dominates	R(T) Kondo anomaly	
Coulomb exchange J _C	Less important		
Strength of 5f delocalization	Weak compared to UTe, increases under pressure	Slight decrease but negative curvature of B _{hf} , S, e ² qQ ; increase of T _{ord} up to 25 GPa with ΔV/V ₀	Experiment: photoemission theory: band-structure calculation within model II (Ref. 42)

low ordered moment of $0.8\mu_B$ are typical features of a band magnet. In contrast, for NpGa₃ we favor the model of a localized magnet with only slight 5f hybridization. The localized model has already been suggested from bulk measurements at ambient pressure.²³

We find further support from a comparison of the volume derivatives of the magnetic ordered moment μ_{ord}, the ordering temperature T_{ord} and the electron density at the nucleus ρ(0) with other compounds. This is shown in Table III. DyAl₂, NpCo₂Si₂, and NpSn₃ are considered as localized 4f or 5f systems, NpAs and NpAl₂ are grouped in the intermediate range and NpOs₂ is classified as a 5f band magnet.²⁹ The positive sign of $-d \ln T_{\text{ord}}/d \ln V$ and the weak volume dependence of μ_{ord} as found for NpGa₃ usually exclude the model of a band magnet.¹¹ Due to the large spin-orbit coupling in localized as well as in itinerant 5f magnets the ordered moment μ_z = μ_B(L_z - 2S_z) is composed of an orbital as well as a spin contribution of opposite sign. In the light actinides the orbital part is in most cases larger than the spin contribution, even in band magnets.³⁹ When pressure is applied to an itinerant 5f magnet the 5f band broadens and the orbital part is quenched much more effectively than the spin contribution. This causes a reduction of the total moment under pressure.⁴⁰ The suppression of the moment and the broadening of the 5f band lead to a decrease of T_{ord}.

For NpGa₃ the slope of $d \ln T_{\text{ord}}/d \ln V = +6$ is comparable to the other localized systems in Table III. In Fig. 7 the saturated magnetic hyperfine field B_{hf}, the ordering temperature T_{ord}, the isomer shift S, the coupling constant e²qQ of the quadrupole interaction, and the b/a ratio (b/a ∝ |dR/d ln T|) are plotted against volume change. The small decrease of μ_{ord} by less than 4% suggests that the 5f states are weakly hybridized between ambient pressure and 9.2 GPa. The negative curvature observed for B_{hf} (see Fig. 7, top) is probably due to the onset of a stronger 5f delocalization above 9 GPa. The ordering temperature shows a linear volume dependence below 10 GPa. This again is a strong indication for (weak) delocalization of 5f electrons. In the systems NpCo₂Si₂ (Ref. 29) and EuAl₂,⁴¹ where delocalization

is not present at all, the ordering temperature rises quadratically (or even faster) with |ΔV/V₀|. In NpGa₃ weak delocalization of 5f electrons causes a reduction of B_{hf} (see Fig. 7, top) and leads to only a linear increase of T_{ord}. Surprisingly the slope of T_{ord} (●, ■) increases at higher pressures (see Figs. 6 and Sec. IV C below). However, the slope of the ordering temperature above 9 GPa has to be treated with caution since it was derived by assuming that the inflection point of the resistance (■) also coincides with T_{ord} in the higher pressure range (see Sec. III C). At present it is unclear if this assumption strictly holds also in the high-pressure regime.

The variation of the electron density ρ(0) at the nucleus with volume derived from the isomer shift gives us a further clue how effectively the 5f states hybridize under pressure. In Refs. 4 and 5 it was suggested that 5f electron delocalization leads to a less effective screening of the outer Np s and p_{1/2} electrons by the 5f electrons and thus to a strong increase of ρ(0). Such a behavior is indeed observed in NpOs₂. This mechanism is supported by theoretical band-structure calculations performed for UTe with varying volume of the unit cell.⁴² According to Ref. 42 pressure-induced 5f delocalization causes a loss of 5f spectral density in real space, i.e., the 5f wave functions are more extended outside of the core region. As a consequence the magnetic moments are reduced. This also leads to a much stronger increase of ρ(0) than observed for localized rare-earth systems such as DyAl₂ and EuAl₂.⁴¹ However, the still weak volume dependence of the isomer shift in NpGa₃ excludes all models assuming a strong 5f delocalization, which would be found in 5f band magnets like NpOs₂ or intermediate valence systems. The negative curvature of the S versus volume curve is a hint that 5f delocalization may become more significant above 9 GPa.

The absolute value of the induced electric quadrupole coupling constant |e²qQ| shows a similar negative curvature in its volume dependence as B_{hf} and S. We suggest that the decrease of |e²qQ|, B_{hf} and S is driven by a slight pressure-induced delocalization of the 5f states. A decrease of these

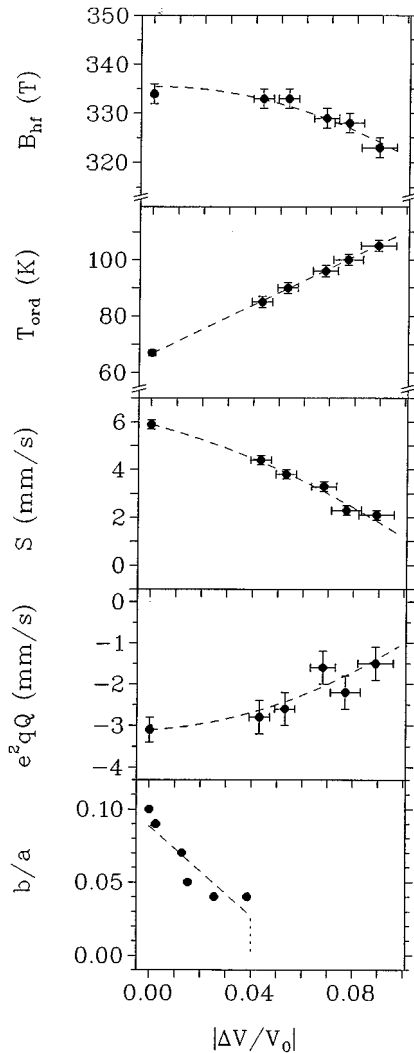


FIG. 7. Magnetic hyperfine field B_{hf} at 4.2 K, ordering temperature T_{ord} , isomer shift S relative to NpAl_2 , quadrupole coupling constant e^2qQ at 4.2 K, and the b/a ratio of the resistance, plotted versus volume change. Since our fitted b/a ratios only reflect the trend of the $dR/d \ln T$ dependence on volume, error bars have been omitted.

parameters has also been observed for NpAs and a similar interpretation has been given.⁴³ For the further discussion we assume, therefore, a weak interaction between the $5f$ moments and the conduction band.

B. Magnetic interactions

In Sec. IV A we ruled out the model of a $5f$ -band magnet. In this section we try to answer by which mechanism μ_{ord} ($1.6\mu_B$) and e^2qQ (-3.1 mm/s) are reduced relative to the free-ion values ($2.6\mu_B$ and ~ -27 mm/s, respectively). For an understanding of the volume dependences of the hyperfine parameters, the magnetic ordering temperature, and of the resistance behavior of NpGa_3 it is crucial to examine the interactions which have been found to be important in actinide systems.^{44,45} Some of these interactions are listed in Table IV.

If we assume localized $5f$ states the values of the isomer shift at all pressures suggest a Np^{3+} configuration with a $5I_4$

Hund's rule ground state.^{4,23,29} The crystal-field (CF) Γ_5 state is compatible with the experimental values of μ_{ord} and e^2qQ at ambient pressure and with μ_{eff} derived from the Curie-Weiss behavior of the magnetic susceptibility.²³ On the other hand, μ_{ord} could partly be quenched by Kondo compensation. As will be discussed below our high-pressure data probably exclude this possibility.

Because of the low value of the induced quadrupole coupling constant $|e^2qQ|$ found in NpGa_3 we neglect the quadrupolar interaction between the $5f$ electrons of neighboring Np atoms and the anisotropy of the magnetic exchange interaction. Both effects can be present when the $5f$ charge distribution is strongly anisotropic. They are assumed to be important, e.g., for the pnictides of the light actinides.⁴⁴ Indeed the Np pnictides NpAs , NpSb , and NpBi show a high value of the induced quadrupole coupling constant [between -29 and -31 mm/s (Ref. 46)]. In contrast for NpGa_3 the absolute value of e^2qQ is below 4 mm/s at all pressures and temperatures investigated. This hints at a weak charge anisotropy. Furthermore NpGa_3 is likely to be only weakly anisotropic in the ferromagnetic phase as has been found for the isostructural NpIn_3 .⁴⁷

The spin-exchange interaction of the $5f$ electrons with the band electrons can either be driven by an antiferromagnetic hybridization exchange or by a ferromagnetic Coulomb exchange.⁴⁵ The Coulomb exchange dominates in the localized rare-earth systems, where no hybridization of the $4f$ electrons is present.⁴⁸ To our knowledge a resistivity Kondo anomaly has never been observed in these systems and is not expected from theoretical models if the Coulomb exchange dominates.^{15,16} The presence of the Kondo anomaly in NpGa_3 therefore suggests that the hybridization exchange is the more important mechanism in our case.

The question arises whether the antiferromagnetic exchange J_h also leads to a Kondo compensation of μ_{ord} ($1.6\mu_B$) relative to the free-ion value ($2.6\mu_B$). This is an alternative mechanism (besides $5f$ delocalization or CF interaction) which may explain the reduction of μ_{ord} . We examine this possibility by comparing the volume dependence of μ_{ord} , T_{ord} , and $|dR/d \ln T|$ with what is expected from the Doniach model.¹³

Model I (Doniach model)

The model is described in the appendix. The increase of T_{ord} and the decrease of μ_{ord} can be explained by assuming that the model parameter J_h/W is below the critical value $J_h/W < (J_h/W)_c$ at ambient pressure and increases with reduced volume, as in CeAg .⁴⁹ However, in contrast to CeAg and CeAl_2 ,¹⁶ in NpGa_3 the resistance anomaly $|dR/d \ln T|$ decreases and finally breaks down at elevated pressure. The volume dependence of T_{ord} and of $|dR/d \ln T|$ can also be understood if $J_h/W > (J_h/W)_c$ at ambient pressure and if J_h/W decreases under pressure. However, this is unlikely, as an estimate shows (see Appendix). Furthermore, a decrease of J_h/W would probably coincide with an increase of μ_{ord} (Ref. 48) in contrast to our observation. We suggest that the saturated moment is reduced rather by CF interaction than by Kondo compensation and that the volume dependence of μ_{ord} and T_{ord} can be explained within model II.

Model II (5f electron delocalization)

To establish an alternative picture for NpGa₃ we compare its pressure behavior with that of UTe.^{42,50} In UTe, T_{ord} increases at low pressures, shows a maximum at ~ 7.5 GPa and decreases at higher pressures. The resistivity anomaly disappears at ~ 4 GPa. According to the theoretical work in Ref. 42, an increase of the hybridization and thus of the magnetic exchange interaction raises T_{ord} . At the same time an enhanced 5f delocalization reduces μ_{ord} with reduced volume, which weakens magnetic order. This competition was proposed to be responsible for the maximum in the T_{ord} versus volume curve of UTe. We invoke the same magnetic mechanism for NpGa₃. We suggest that the 5f states of NpGa₃ are less hybridized than in UTe so that T_{ord} increases even up to 25 GPa and shows a maximum at still higher pressures. The relatively weak 5f delocalization was already concluded from the volume dependence of B_{hf} , T_{ord} , and S in Sec. IV A. Unfortunately, to our knowledge the resistivity anomaly has never been investigated theoretically within models including 5f delocalization effects. We suggest that the decrease of $|dR/d \ln T|$ with reduced volume, also observed in UTe,⁵⁰ NpSb,⁵¹ and NpAs,⁵² might be driven by increasing charge fluctuations of the 5f states. Since we expect a small increase of the 5f delocalization with reduced volume in NpGa₃ (see Sec. III A), these fluctuations certainly play a major role. However, they are underestimated by the Schrieffer-Wolff transformation,^{53,54} on which model I is based. Therefore, it is not surprising that model I fails to describe certain U or Np systems. Since the 5f states in compounds of the light actinides are usually more delocalized than the Ce 4f electrons,⁵⁵ it is consistent to assume that model I is a good description for Ce intermetallics but not for NpGa₃ or UTe.

C. Magnetic phase diagram

In Fig. 6 the ordering temperature derived from the Mössbauer (●) and resistance (■) data, and the temperature where the sharp resistance drop (Δ) occurs are plotted against volume change. The figure also shows our suggestion for the magnetic phase diagram. The magnetic hyperfine fields as a function of temperature (see Fig. 3), the resistance drop (Δ) and the inflection point (■) at the ordering temperature (see Fig. 5) are the main features on which the phase diagram is based.

If we took the Mössbauer results alone we would be tempted to argue that the absence of the smaller hyperfine field above 50 K and under pressure (see Fig. 3) indicates the disappearance of the antiferromagnetic (AF) phase. This was observed at ambient pressure with applied magnetic field rather than pressure.³² In our case we would expect the resistance drop (Δ) to shift towards T_{ord} (●, ■), since such a drop is usually characteristic of a ferromagnetic phase transition.⁵⁶ However, the temperature of the drop (Δ) is below T_{ord} (●, ■) by more than 15 K at all pressures and is constant up to 10 GPa, whereas T_{ord} (●, ■) strongly rises with increasing pressure. Moreover, above 5 GPa the inflection point (■) at the onset of magnetic order is highly unusual for a ferromagnetic phase transition. This behavior is rather characteristic of an antiferromagnetic transition, which leads to a larger unit cell of the crystal (supercell) and may

cause a band gap at the Fermi surface.⁵⁷ A reduction of the lattice symmetry can be caused by an amplitude modulation of the magnetic moments or by an antiferromagnetic arrangement of the spins with moments of *one* amplitude. The Mössbauer results exclude the first possibility, since the fits with only *one* hyperfine field are in good agreement with the data. Our measurements at elevated pressure furthermore reveal that in the AF phase the ordered moment is not reduced anymore, in contrast to the situation at ambient pressure. This increased ordered moment and the different resistance behavior at the phase transition above 0.2 GPa suggests that the spin arrangement in the AF phase changes under pressure.

The low-temperature drop of the resistance at elevated pressure could either be due to a reduction of the spin-wave scattering with decreasing temperature in the AF phase³⁵ or it could be caused by an antiferro- to ferromagnetic (AF-F) transition similar to the situation at ambient pressure. Since the temperature (Δ) where the drop appears shows no correlation to the increase of T_{ord} (●, ■) with pressure we favor the second alternative.

V. CONCLUSIONS

We suggest that the different pressure behavior of NpGa₃ with respect to the Kondo systems CeAl₂ and CeAg is due to a larger delocalization of the Np 5f electrons compared to the Ce 4f electrons. For this reason the Doniach picture does not apply. On the other hand, because of the still small pressure variation of the isomer shift and of the ordered moment and due to the increase of T_{ord} up to 25 GPa the degree of 5f delocalization is lower than in UTe.

Our suggestions concerning the relevance of several 5f interactions are summarized in Table IV. The strength of the 5f delocalization could be studied by a photoemission experiment. A comparison of the photoemission results with CeAg, CeAl₂, and UTe may provide a test for our prediction that the 5f states of NpGa₃ are more delocalized than the Ce 4f states but less hybridized than in UTe. Furthermore, a theoretical investigation within model II (Ref. 42) of the 5f delocalization and of the 5f screening effect on the electron density at the nucleus would provide a deeper understanding of the dependence of the isomer shift on 5f delocalization. Theoretical investigations could also examine whether the decrease of the size of the induced quadrupole interaction and of the resistivity slope $|d\rho/d \ln T|$ with reduced volume can be explained within model II by a slight increase of the 5f charge fluctuations.

A high-pressure resistivity study on the isostructural but possibly more localized compounds NpIn₃ (Ref. 5) and NpSn₃ (Ref. 10) would show whether these systems can be described within the Doniach picture. An inelastic neutron experiment would be able to verify whether the CF model which is usually applied to localized systems is also a proper approximation for NpGa₃. The question how anisotropic 5f hybridization influences the CF states could be examined by theory.^{58,59}

Our suggestion of a magnetic phase diagram should be checked by elastic neutron diffraction. Unfortunately up to now high-pressure neutron experiments are not available for Np compounds for safety reasons. AC susceptibility mea-

surements at high pressure might provide a test for our suggestion that the AF-F transition is still present at elevated pressure.

ACKNOWLEDGMENTS

We wish to thank M. S. S. Brooks and G. H. Lander for illuminating discussions. The high-purity Np metal required for the fabrication of NpGa₃ was made available in the framework of a collaboration with the Lawrence Livermore and Los Alamos National Laboratories and the U.S. Department of Energy. This work was funded in part by the German Federal Minister for Research and Technology (BMFT) under Contract No. KA3TUM/A.4-K03. Support given to some of us (S.Z., V.I., D.B., J.C.W.) by CEC is also acknowledged.

APPENDIX: DESCRIPTION OF MODEL I AND ITS CONSEQUENCES FOR NpGa₃

Model I

In extended versions of the Doniach model which are applied to Ce and actinide systems the competition between magnetic order and Kondo effect is controlled by the parameter J_h/W , where W is the bandwidth at the Fermi level and J_h is the exchange parameter due to the hybridization between the $5f$ and conduction electrons.¹⁵ The hybridization exchange parameter J_h is given by $J_h = |V_{kF}|^2 U / [E_{5f}(E_{5f} + U)]$.¹⁵ V_{kF} is the corresponding hybridization matrix element, U the Anderson correlation energy, and E_{5f} is the energy of the $5f$ electrons relative to the Fermi level. In this model the anisotropy of J_h and V_{kF} , i.e., their dependence on the magnetic quantum number of the electronic state of the ion is neglected. Furthermore J_h is derived by the application of the Schrieffer-Wolff transformation to the Anderson Hamiltonian, which might underestimate $5f$ charge fluctuations.^{15,53,54}

For many Ce compounds the pressure variation of T_{ord} and the Kondo temperature can be well explained by assum-

ing that the model parameter J_h/W increases under pressure.^{60,49} If J_h/W is smaller than a critical value $(J_h/W)_c$ then T_{ord} rises at low pressures, goes through a maximum and decreases at sufficiently high pressures. In this case a resistivity Kondo anomaly can appear under pressure as, e.g., in CeAg or CeCu₂Ge₂. If J_h/W is above $(J_h/W)_c$ at ambient pressure, a decrease of T_{ord} and an increase of $|d\rho/d \ln T|$ should occur under pressure as in CeAl₂.¹⁶

Estimation of the volume dependence of J_h/W

It is discussed why we expect the model parameter J_h/W to increase under pressure (see Sec. IV B, model I). According to Ref. 2 in AnX₃ compounds the $5f$ hybridization V_{kF} is mainly determined by the mixing V_{pf} between the $5f$ and the ligand p electrons. Thus to estimate the volume dependence of J_h/W we can replace V_{kF} by V_{pf} . According to a combined muffin-tin theory with transition pseudopotentials a general matrix element $V_{ll'm}$ has been derived,⁶¹ which describes the hybridization between orbitals of angular momenta l, l' ($l, l' = 0, 1, 2, 3$ for s, p, d, f orbitals, respectively) with the symmetry m of the bond ($m = 0$ for σ bond, $m = 1$ for π bond, etc.). If we assume m to be pressure independent $V_{ll'm}$ shows the proportionality $V_{ll'm} \propto d^{-(l+l'+1)}$ with the interatomic distance d . Using this for NpGa₃ we arrive at the volume dependence $V_{pf} \propto V^{-5/3}$. The width W of the conduction band scales with $V^{-5/3}$ for d electrons or a lower power of $(1/V)$ if only s and p electrons form the conduction band. If E_{5f} and U are pressure independent, we obtain $J_h/W \propto V^{-5/3}$. Thus if (J_h/W) was supposed to decrease under pressure, the factor $U/[E_{5f}(E_{5f} + U)]$ would have to overcompensate the increase by $V^{-5/3}$. This would be possible, if the $5f$ energy decreases strongly relative to the Fermi level. It would mean that the $5f$ electrons become even more localized under pressure. As another possibility, the correlation parameter U could strongly decrease. This, however, would lead to a considerable $5f$ delocalization. Both mechanisms are in contradiction to our discussion in Sec. IV B. Therefore we expect J_h/W to increase when volume is reduced.

¹V. Sechovsky and L. Havela, in *Ferromagnetic Materials*, edited by E. P. Wohlfarth and K. H. J. Buschow (North-Holland, Amsterdam, 1988), Vol. 4, Chap. 4, pp. 310–491.

²D. D. Koelling, B. D. Dunlap, and G. W. Crabtree, *Phys. Rev. B* **31**, 4966 (1985).

³*Ferromagnetic Materials* (Ref. 1), pp. 380–391.

⁴J. Gal, I. Yaar, S. Fredo, I. Halevy, W. Potzel, S. Zwirner, and G. M. Kalvius, *Phys. Rev. B* **46**, 5351 (1992).

⁵S. Zwirner, W. Potzel, J. C. Spirlet, J. Rebizant, J. Gal, and G. M. Kalvius, *Physica B* **190**, 107 (1993).

⁶J. P. Sanchez, M. N. Bouillet, E. Colineau, A. Blaise, M. Amanowicz, P. Burette, J. M. Fournier, T. Charvolin, and J. Larroq, *Physica B* **186-188**, 675 (1993).

⁷M. R. Norman, S. D. Bader, and H. A. Kierstead, *Phys. Rev. B* **33**, 8035 (1986).

⁸R. J. Trainor, M. B. Brodsky, B. D. Dunlap, and G. K. Shenoy, *Phys. Rev. Lett.* **37**, 1511 (1976).

⁹M. R. Norman and D. D. Koelling, *Phys. Rev. B* **33**, 3803 (1986).

¹⁰G. M. Kalvius, S. Zwirner, U. Potzel, J. Moser, W. Potzel, F. J. Litterst, J. Gal, S. Fredo, I. Yaar, and J. C. Spirlet, *Phys. Rev. Lett.* **65**, 2290 (1990).

¹¹J. M. Fournier, *Physica B* **130**, 268 (1985).

¹²S. H. Liu, in *Handbook of the Physics and Chemistry of Rare Earths*, edited by K. A. Gschneidner, L. Eyring, G. H. Lander, and G. R. Choppin (North-Holland, Amsterdam, 1993), Vol. 17, Chap. 111, pp. 95–97.

¹³S. Doniach, in *Valence Instability and Related Narrow-Band Phenomena*, edited by R. D. Parks (Plenum, New York, 1977), pp. 169–176; *Physica B* **91**, 231 (1977).

¹⁴N. B. Brandt and V. V. Moshchalkov, *Adv. Phys.* **33**, 373 (1984).

¹⁵B. Coqblin and J. R. Schrieffer, *Phys. Rev.* **185**, 847 (1969).

¹⁶B. Coqblin, in *Magnetism of Metals and Alloys*, edited by M. Cyrot (North-Holland, Amsterdam, 1982), Chap. 3, pp. 339–358.

¹⁷T. Endstra, G. J. Nieuwenhuys, and J. A. Mydosh, *Phys. Rev. B* **48**, 9595 (1993).

- ¹⁸J. D. Thompson and J. M. Lawrence, in *Handbook of the Physics and Chemistry of Rare Earths* (Ref. 12), Vol. 19, Chap. 133, pp. 383–478.
- ¹⁹O. Vogt and K. Mattenberger, in *Handbook of the Physics and Chemistry of Rare Earths* (Ref. 12), Vol. 17, Chap. 114, pp. 344.
- ²⁰E. Pleska, Ph.D. thesis, Université Joseph Fourier Grenoble, 1990.
- ²¹T. M. Holden, J. A. Jackman, W. J. L. Buyers, K. M. Hughes, M. F. Collins, P. de V. DuPlessis, and O. Vogt, *J. Magn. Magn. Mater.* **63-64**, 155 (1987).
- ²²B. Frick, J. Schoenes, and O. Vogt, *J. Magn. Magn. Mater.* **47-48**, 549 (1985).
- ²³M. N. Bouillet, T. Charvolin, A. Blaise, P. Burlet, J. M. Fournier, J. Larroque, and J. P. Sanchez, *J. Magn. Magn. Mater.* **125**, 113 (1993).
- ²⁴G. Huber, K. Syassen, and W. B. Holzapfel, *Phys. Rev. B* **15**, 5123 (1977).
- ²⁵H. K. Mao, P. M. Bell, J. W. Shaner, and D. J. Steinberg, *J. Appl. Phys.* **49**, 3276 (1978).
- ²⁶U. Benedict and C. Dufour, *High Temp. High Pressure* **16**, 501 (1984).
- ²⁷B. Bireckoven and J. Wittig, *J. Phys. E* **21**, 841 (1988).
- ²⁸J. Moser, W. Potzel, B. D. Dunlap, G. M. Kalvius, J. Gal, G. Wortmann, D. J. Lam, J. C. Spirlet, and I. Nowik, in *Physics of Solids Under High Pressure*, edited by J. S. Schilling and R. N. Shelton (North-Holland, New York, 1981), p. 271.
- ²⁹W. Potzel, G. M. Kalvius, and J. Gal, in *Handbook of the Physics and Chemistry of Rare Earths* (Ref. 12), Vol. 17, Chap. 116, pp. 578.
- ³⁰F. Birch, *Phys. Rev.* **71**, 809 (1947).
- ³¹S. Zwirner, Diploma thesis, Technische Universität München, 1989.
- ³²J. P. Sanchez and E. Colineau, in *Proceedings of XXX Zakopane School of Physics: Condensed Matter Studies by Nuclear Methods*, edited by K. Tomala and E. A. Görlich (Stabill, Krakow, 1995), p. 153.
- ³³S. Ofer, I. Nowik, and S. G. Cohen, in *Chemical Applications of Mössbauer Spectroscopy*, edited by V. I. Goldanskii and R. H. Herber (Academic, New York, 1968).
- ³⁴B. D. Dunlap and G. M. Kalvius, in *Handbook of the Physics and Chemistry of the Actinides*, edited by A. J. Freeman and G. H. Lander (North-Holland, Amsterdam, 1985), Chap. 5, p. 367.
- ³⁵J. M. Fournier and E. Gratz, in *Handbook of the Physics and Chemistry of Rare Earths* (Ref. 12), Vol. 17, Chap. 115, pp. 419–424.
- ³⁶M. Amanowicz, Ph.D. thesis, Université Joseph Fourier Grenoble, 1995.
- ³⁷D. E. Hegland, S. Legvold, and F. H. Spedding, *Phys. Rev.* **131**, 158 (1963).
- ³⁸*Handbook of the Physics and Chemistry of the Actinides* (Ref. 34), pp. 387–389.
- ³⁹G. H. Lander, M. S. S. Brooks, and B. Johansson, *Phys. Rev. B* **43**, 13 672 (1991).
- ⁴⁰M. S. S. Brooks, *Physica B* **190**, 55 (1993).
- ⁴¹A. Gleissner, W. Potzel, J. Moser, and G. M. Kalvius, *Phys. Rev. Lett.* **70**, 2032 (1993), and references therein.
- ⁴²B. R. Cooper, Q. G. Sheng, U. Benedict, and P. Link, *J. Alloys Compounds* **213/214**, 120 (1994).
- ⁴³U. Potzel, Ph.D. thesis, Technische Universität München, 1987.
- ⁴⁴G. H. Lander and P. Burlet, *Physica B* **215**, 7 (1995).
- ⁴⁵Q. G. Sheng and B. R. Cooper, *J. Appl. Phys.* **69**, 5472 (1991).
- ⁴⁶M. N. Bouillet, Ph.D. thesis, Université Joseph Fourier, Grenoble, 1993.
- ⁴⁷E. Colineau, A. Blaise, P. Burlet, J. P. Sanchez, and J. Larroque, *Physica B* **206-207**, 528 (1995).
- ⁴⁸P. Monachesi and A. Continenza, *Phys. Rev. B* **47**, 14 622 (1993).
- ⁴⁹A. Eiling and J. S. Schilling, *Phys. Rev. Lett.* **46**, 364 (1981).
- ⁵⁰P. Link, U. Benedict, J. Wittig, and H. Wühl, *J. Phys. Condens. Matter* **4**, 5585 (1992).
- ⁵¹M. Amanowicz, D. Braithwaite, V. Ichas, U. Benedict, J. Rebizant, and J. C. Spirlet, *Phys. Rev. B* **50**, 6577 (1994).
- ⁵²V. Ichas, D. Braithwaite, S. Zwirner, M. Amanowicz, J. C. Spirlet, J. Rebizant, and U. Benedict (unpublished).
- ⁵³J. R. Schrieffer and P. A. Wolff, *Phys. Rev.* **149**, 491 (1966).
- ⁵⁴P. Fulde, in *Electron Correlations in Molecules and Solids*, edited by M. Cardona, P. Fulde, K. v. Klitzing, H.-J. Queisser, and Managing Editor H. K. V. Lotsch (Springer-Verlag, New York, 1991), Chap. 13, pp. 280–282.
- ⁵⁵Q. G. Sheng, B. R. Cooper, and S. P. Lim, *J. Appl. Phys.* **73**, 5409 (1993).
- ⁵⁶T. Kasuya, *Prog. Theor. Phys.* **16**, 45 (1956).
- ⁵⁷J. Jensen and A. R. Mackintosh, *Rare Earth Magnetism* (Oxford Science, Oxford, 1991), pp. 281–284.
- ⁵⁸P. M. Levy and S. Zhang, *Phys. Rev. Lett.* **62**, 78 (1985).
- ⁵⁹B. R. Cooper, J. M. Wills, N. Kioussis, and Q. G. Sheng, *J. Phys. (Paris) Colloq.* **49**, C8-463 (1988).
- ⁶⁰*Handbook of the Physics and Chemistry of Rare Earths* (Ref. 18), pp. 448–454.
- ⁶¹W. A. Harrison and G. K. Straub, *Phys. Rev. B* **36**, 2695 (1987).